

Noise residuals for GW150914 using maximum likelihood and numerical relativity templates

Andrew D. Jackson,^a Hao Liu,^{b,c} and Pavel Naselsky^b

^aThe Niels Bohr International Academy, Blegdamsvej 17, DK-2100 Copenhagen, Denmark

^bThe Niels Bohr Institute & Discovery Center, Blegdamsvej 17, DK-2100 Copenhagen, Denmark

^cKey Laboratory of Particle and Astrophysics, Institute of High Energy Physics, CAS, 19B YuQuan Road, Beijing, China

E-mail: jackson@nbi.dk, liuhao@nbi.dk, naselsky@nbi.dk

Abstract.

We reexamine the results presented in [1] in which the properties of the noise residuals in the 40 ms chirp domain of GW150914 were investigated. This paper confirmed the presence of strong (i.e., about 0.80) correlations between residual noise in the Hanford and Livingston detectors in the chirp domain as previously seen by [2] when using a numerical relativity template given in [3]. It was also shown in [1] that a so-called maximum likelihood template can reduce these statistically significant cross-correlations. Here, we demonstrate that the reduction of correlation and statistical significance is due to (i) the use of a peculiar template with extreme spin (0.977), which is qualitatively different from the properties of GW150914 originally published by LIGO, (ii) a suspicious MCMC chain, (iii) uncertainties in the matching of the maximum likelihood (ML) template to the data in the Fourier domain, and (iv) a biased estimation of the significance that gives counterintuitive results. We show that rematching the maximum likelihood template to the data in the 0.2 s domain containing the GW150914 signal restores these correlations at the level of 60% of those found previously [1]. With necessary corrections, the probability given in [1] for the residual correlation will decrease by more than one order of magnitude. Since the ML template is itself problematic, results associated with it are illustrative rather than final.

Contents

1	Introduction and Motivation.	1
2	The “maximum likelihood” template	3
2.1	Parameters of the ML-template	3
2.2	Self-contradictions in the MCMC chain	4
2.3	Degrees of freedom, fluctuations in the SNR, and residual correlations	5
3	Hanford-Livingston noise residuals and their cross-correlations	5
4	Evaluation of the significance of residual correlations	8
4.1	More robust estimation of the significance of residual correlation	8
4.2	Calculations with the old estimator	10
4.2.1	Example of varying the window position	11
4.2.2	Significance estimation with 9 window average	11
4.2.3	Investigation of the RMS peaks	11
5	Uncertainties in the maximum likelihood method	13
6	Conclusion	14
7	Acknowledgement.	14
A	The Pearson cross-correlator for LIGO noise	15
B	A toy model of residuals	15
B.1	Residuals correlations for the high amplitude case.	17

1 Introduction and Motivation.

Knowledge of the properties of noise in the LIGO Hanford and Livingston data sets is crucial for verification of the methods used to determine the physical nature and quantitative details of the GW150914 event and all subsequent events [3]. In practice, the maximum likelihood method used in [1] to analyze the GW events effectively assumes that the noise is both stationary and Gaussian. The validity of these crucial assumptions can be tested by considering the cross-correlations of the Hanford and Livingston noise residuals, which should be at the level of chance correlations. In [2] we explored the assumption of uncorrelated Hanford/Livingston noise residuals for GW150914 by considering a windowed Pearson cross-correlator (see Appendix A for more details). Significant abnormal correlations were found.

Using a numerical relativity (NR) template [3], we identified [2] three 40 ms domains of significant noise correlation in a 0.2 s record¹: the chirp domain (16.39-16.43s) with a Hanford/Livingston cross-correlation of 0.80, the precursor domain (16.27-16.31s) with a cross-correlation of 0.60, and the echo domain (16.47-16.51s) during ring-down with a cross-correlation of similar amplitude [2]. Taken

¹The strain data for a 0.2 s time interval including GW150914 and the NR template are available at the LIGO Open Science Center (LOSC). In the present paper, time positions are measured relative to the 32 seconds centered at GPS time 1126259462, a convention established in some of the files of the initial LOSC release. For example, the peak amplitude of the GW150914 event occurs at approximately 16.42 seconds.

together, these results are not consistent with the assumption of uncorrelated noise residuals under Gaussian and stationary assumptions. Recently, this result was confirmed using the same NR template and 0.2s time interval in [1]. However, the authors of this paper also claim that the strong abnormal residual correlations discovered in [2] can be reduced significantly in the chirp domain by using an alternative ML template. We cannot with certainty exclude the possibility that some template in LIGO’s models of binary black hole mergers can locally reduce residual correlations. While we investigated this question in [1], we did not consider specific templates involving black holes with extreme spins. Given that in the ML template, one of its participating black hole has a spin indistinguishably close to the maximum possible value of 1, the ML template adopted in [1] is an example of one such extreme template.

Clearly, independent verification of the methods and results of LIGO, such as [1], is a matter of importance for our understanding of black hole physics. Especially since, according to ref. [37] in [3], the NR template used by LIGO is SXS:BBH:0305 which has on-axis spins of +0.33 and -0.44 is almost identical to a zero spin template. In sharp contrast, the ML template discussed in [1] involves a black hole with extreme spin — almost the physical limit. This difference has important consequences. Unlike low-spin black holes, high-spin Kerr black holes cannot be formed at early stages in the evolution of the Universe as so-called primordial black holes. The black holes suggested by the results of [1] would rather indicate that the black holes involved have a stellar origin from very massive stars. Even given the stellar origin of such black holes, the extreme spin would appear to be challenging.

We also point out that the cleaned (i.e., bandpassed and notch-filtered) strain data used by [1] is essentially identical to ours [2, 4]. Using a bandpass window of $35 \leq f \leq 350$ Hz, none of the 37240 templates considered in [5] (from which the ML template is extracted) can reduce the precursor effect observed during the first 0.1s of GW150914. (This leads to a cross-correlation of 0.60 between H/L residuals.) Indeed, in this time window the NR template, like all other templates filtered from $35 \leq f \leq 350$ Hz, is almost negligible in comparison with noise.

Our goal here is to reevaluate the methods and results of [1] with regard to their claims about the noise residuals for GW150914. We will first show that the matching of the ML template to the data depends on the estimator assumed. In [1] the quantity to be optimized is a complex overlap function (of Hanford and Livingston strain data) with the same overall phase for each template. (See Table 1 and its caption.) This constraint on the phase proves to be crucial for introducing an effective shift of the peak position in the chirp domain. Consequently, it plays a major role in decreasing the residual noise correlation. Second, calculation of the SNR parameter involves a power spectral density (PSD) obtained from a time interval that is nearly 4 orders of magnitude larger than the length of the most significant GW domain (1040s versus 0.2s). The validity of this approach critically depends on the assumptions that the noise is stationary and Gaussian. Neither assumption is true. On the other hand, the equal-time comparison used for matching with the Pearson estimator of eq. (A.2) does not depend on any such assumptions. It can be applied safely for short (e.g., 0.2s) records. In general, it is important to bear in mind that the implementation of any statistical concepts, such as chance correlations, for the estimation of the significance of noise cross-correlations needs to be performed with care. Due to the non-stationarity and non-Gaussianity of the noise residuals, all such estimates can be misleading. (This point will be illustrated in Sections 4-5.) We emphasize that we do not regard such assumptions as safe and have avoided them in [1] and [2]. Nevertheless, we will from time to time be forced to assume stationarity and Gaussianity in the interests of following the methods of [1].

The outline of the paper is as follows. In Section 2, we briefly review the maximum likelihood approach and the corresponding templates as provided in [5] and used in [1]. In Section 3, we consider the residuals and their correlations for both this template and for the NR template. The significance of the residual correlations is estimated in Section 4. Since we regard the ML template itself as unsatisfactory, our primary focus is on how to correct [1] in order to obtain unbiased estimations. We investigate some

uncertainties in the ML method in Section 5, and a brief discussion of the results is given in Section 6.

While this paper is largely concerned with residual correlations, the following should be kept in mind: The presence of statistically significant correlations in the Hanford and Livingston residuals is sufficient to eliminate any proposed waveform (e.g., the NR template of [3]) from further consideration. The absence of such residual correlations does *not* provide any evidence that the proposed waveform is correct.

2 The “maximum likelihood” template

2.1 Parameters of the ML-template

In Table 1, we summarize the parameters of the ML template used by [1], which was produced in [5].

No.	Name	Old value	New value
1	ra (α)	1.5730257	2.1140412
2	dec (δ)	-1.2734810	-1.2518563
3	distance (d_L)	476.7564547	527.0627598
4	inclination (ι)	2.9132713	3.0021228
5	mass1 (m_1)	39.0257656	38.4900335
6	mass2 (m_2)	32.0625631	32.3104771
7	polarization (ψ)	5.9925231	2.6053099
8	spin1_a (a_1)	0.9767961	0.9635978
9	spin1_azimuthal (θ_1^a)	3.6036952	4.7164805
10	spin1_polar (θ_1^p)	1.6283548	1.9250337
11	spin2_a (a_2)	0.1887608	0.2894704
12	spin2_azimuthal (θ_2^a)	3.4359460	2.0230135
13	spin2_polar (θ_2^p)	2.4915268	0.7928019
14	tc (from 1126259462)	0.4175646	0.4151170
15a	coa_phase	0.6883212	N/A
15b	phase_shift ϕ_0	-0.9155276	1.7576289
15c	summed phase	-0.2272064	1.7576289
	SNR	24.36169	24.33653

Table 1. The parameters of the ML template for GW150914 used by [1]. The large number of digits is especially important for “tc” in order to ensure that the uncertainty in positioning is much less than the possible ± 10 ms delay in the arrival time. The ML parameters (in the column “Old values”) were taken from [5]. During the preparation of this work, however, all of these parameters were updated online [6], but [1] used only the old values. Nevertheless, we append the new values for this table which involve relative changes in the parameters ranging from 2% to 200%. In spite of these changes, the resulting templates are almost identical. In [1], the final parameter (15a) is unused in the Markov Chain Monte Carlo (MCMC) process. Its value must be combined with the externally determined ϕ_0 (15b) to give the summed phase (15c). The respective SNRs are shown in the final row. Although they are not significantly different, the original template has a slightly higher SNR. We prefer the old template in the following analysis, not only because of the higher SNR but also because this is precisely the template used by [1].

Table 1 is characterized by 14 parameters that are actively involved in the MCMC optimization and a single parameter (either coa_phase or ϕ_0) that is determined a posteriori. During the random walk, ϕ_0 is a meaningless random number. When the MCMC process is finished, a new estimation will be given

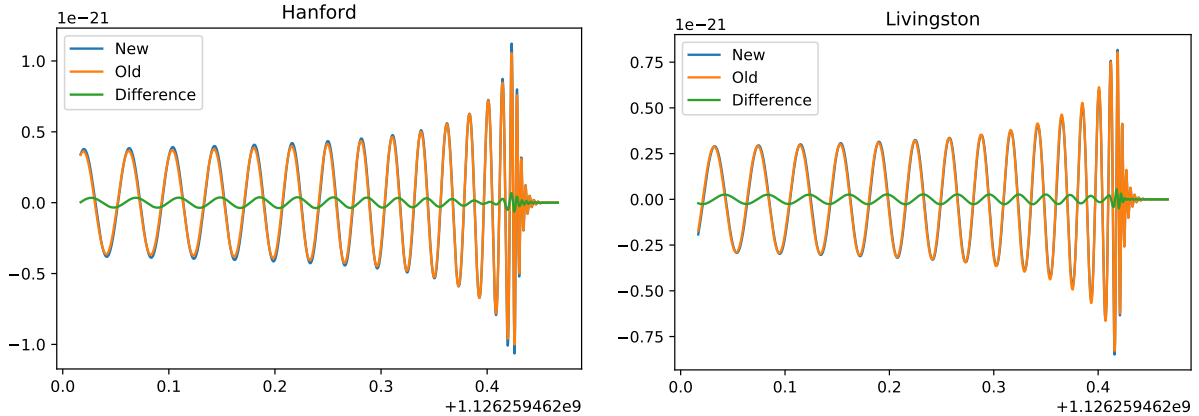


Figure 1. Left panel: Comparison of the old and new templates from Table 1 for Hanford. Right panel: The same for Livingston. The green line is the difference between the old and new templates.

as ϕ_0 so that the final template is

$$\tilde{h}(\theta', \phi_0) = \tilde{h}^0(\theta') e^{i\phi_0}. \quad (2.1)$$

Here, h^0 is the template with $\phi_0 = 0$, and θ' represents the 15 parameters including random ϕ_0 .

Note that, during the preparation of this work, all of the MCMC parameters were updated online [6], but [1] still uses the old values. In Figure 1 we show the old and new templates from Table 1. Although the variations in the parameters themselves range from 2 to 200% and the change in the summed phase ϕ_0 is large, the differences in the time domain morphology are quite small. Moreover, the two templates have almost identical SNRs with a relative variation 0.1%, which is negligible given the magnitude of the noise. This is a clear reflection of strong degeneracy in the parameters². Note in particular that the 2.4 ms in the time shift, t_c , is actually remarkably large. (In this regard, see Figure 1 below.) These differences between the old and new parameters immediately tell us that an expensive ML approach has little scientific merit in determining the possible nature of black hole binaries in events like GW150914. Although the entire ML approach employed in [5] is of questionable value, we will simply take the ML template used by [1] for some further analysis.

Normally, for an MCMC chain, the ML point is asymptotically a best fit point, whereas other points are random walks and can not be regarded as properly fitted. In fact, even the ML point is not a genuine best fit point, because when the MCMC approach is re-run, a new ML point will be generated, which is normally *not* the previous one. This is excellently illustrated by the two columns in Table 1 for the new and old parameters: each of them is the ML point for its own round, but they give significantly different parameters. On the other hand, a fitting procedure, if possible, can give the unique best fit. In the case of two detectors like GW150914, the projection parameters (rows 1, 2, 3, 4, 7, 14, 15 in Table 1) can be related to the matching (fitting) parameters (amplitudes, phases, arrival times) by a physical connection, as shown by [8]. For two detectors, the number of degrees of freedom for matching is less than the number of physical parameter, a re-matching procedure can be applied to the points in the MCMC chain to improve the matching with data. This will be done below.

2.2 Self-contradictions in the MCMC chain

The ML template presented in [1] should be accompanied by a presentation of the distribution of the parameters in the MCMC chain. The purpose is to check whether or not the values of the ML template, as

²These degeneracies have been discussed in [7]. See, for example, the left panel of Figure 7 there.

well as other templates with highest likelihoods, are consistent with the distributions given by the whole converged MCMC chain. Such a test indicates, that the ML template is very special in the MCMC chain. By simply reading the 37240 points of the chain used by [1], we have constructed the scatter plot of the spin1 amplitude versus log-likelihood shown in Figure 2. One can see that most of these templates have low spins. However, the ML template has extreme spin of $a_1 = 0.977$ that almost hits the boundary of allowed priors that ranges from 0 to 0.99 [5], and is greater than 99.6% of the chain templates, i.e., the parameters given by ML template deviate significantly from those of the main chain. A similar situation is seen for the celestial longitude (α), which is also shown in Figure 2. Moreover, both phenomena can be seen in the new chain as well.

All templates shown in Figure 2 have relatively high likelihoods, and the templates with highest likelihoods (including the ML template) are expected to have a posterior distribution consistent with that of the main chain. If the above high-spin anomaly were found for the single ML template, then one may consider solving the problem by excluding this template. However, this is not the case: For example, all 8 templates of highest likelihoods have spins that are in the top 12.5% (see the colored crosses in Figure 2), which has a probability of $\approx 6 \times 10^{-8}$. For the 1024 templates of highest likelihoods, 231 of them are in the same region, which corresponds to a probability of $\approx 2 \times 10^{-19}$. Thus the inclusion of more templates with highest likelihood quickly sharpens this problem rather than alleviating it. This raises concern about the approach of [1], not only for using a single ML template, but also for the correctness of favoring higher and higher likelihoods in their MCMC realization.

2.3 Degrees of freedom, fluctuations in the SNR, and residual correlations

In [1], each point in the MCMC chain corresponds to one template. The 15th parameter of the template (see Table 1) is determined by matching to the strain data with all other parameters fixed. However, a proper matching should contain 6 degrees of freedom (DOF): position, amplitude, and phase for each detector. As a quick consistency check, we continue to use the code of [1] but add a full matching of all 6 DOF using their pyCBC package. Our aim is to focus only on the change from 1 to 6 DOF. The corresponding residual correlations for all 37240 templates in the 16.39s – 16.43s window are plotted in the left panel for 1 DOF and right for 6 DOF. We see that, a partial 1 DOF matching (as adopted in [1]) leads to residual correlations with large fluctuations even though all templates are within $\pm 0.5\%$ relative variation of the SNR. The range of fluctuations is significantly reduced by a full 6 DOF matching but is still large. Therefore, the templates in the MCMC chain tend to produce residual correlation with fluctuations that are large in comparison with the small variations in SNR. Such large fluctuations may not be physically meaningful.

3 Hanford-Livingston noise residuals and their cross-correlations

In Table 1, 8 of the 14 parameters (except the coalescence phase) describe intrinsic properties of the Black Hole binary. These include the mass, spin amplitude, and polar/azimuthal angles for each black hole. The remaining 6 parameters are related to the projection of GW onto detectors. A straightforward matching for 2 detectors will also use 6 parameters including the arrival time, amplitude and phase at each detector. These 6 parameters can be translated into the GW projection parameters. Therefore, for 2 detectors, either way (ML or straightforward matching) has the same number of free parameters for the GW projection. For $n > 2$ detectors, a straightforward matching requires more parameters than there can be, and the projection procedure must be constrained properly. Thus, a ML approach using 15 parameters can be more convenient for $n > 2$ detectors even if each point in the chain is unmatched. However, for two detectors like GW150914, there is no such constraint. Each point in the MCMC chain is “unmatched” and should be “rematched”.

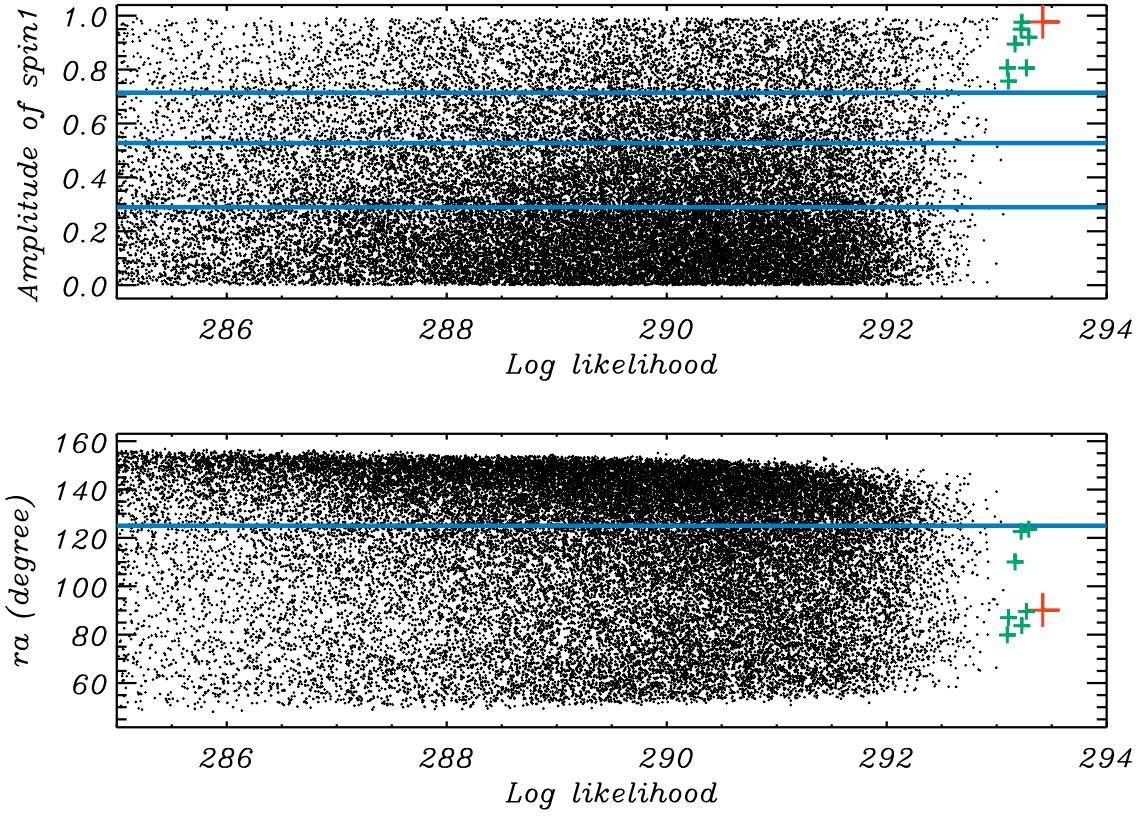


Figure 2. *Upper:* Scatter plot of the spin1 amplitude versus the log-likelihood. The blue lines are 1/2 (median), 1/4 and 1/8 splits of all templates. *Lower:* the same for ra, with the blue line for median split. Red cross for the ML template, and green crosses for the next 7 highest likelihood templates. Data from the MCMC chain used by [1].

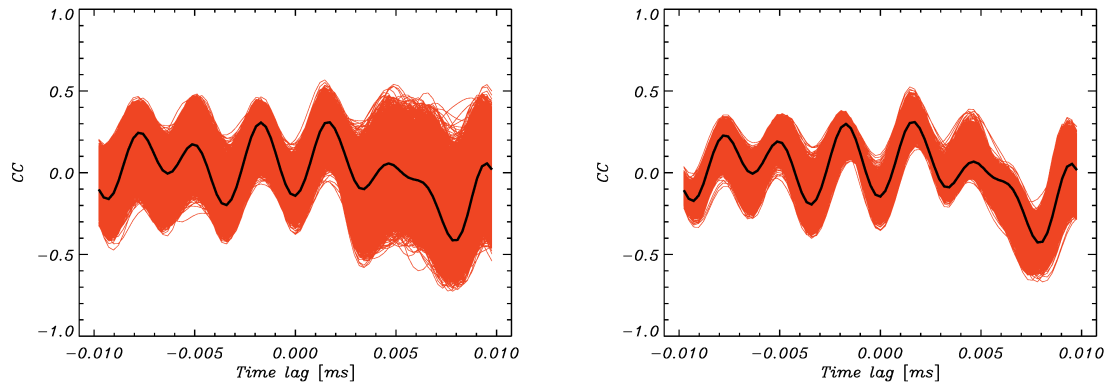


Figure 3. *Left:* Residual correlations for region 16.39s–16.43s for all 37240 templates in the MCMC chain. The one for ML template in black. *Right:* Same as left but each template is matched by 6 DOF instead of 1 DOF.

Before proceeding to the residual correlations, it is useful to look at two distinct methods for matching GW templates to the strain data. The most important consideration for the rematching of templates is the non-stationarity of the GW signal. For the template parameters given in Table 1, the frequency of the GW emitted during the inspiral exceeds the low frequency of the band-pass filter $f_{\min} \simeq 30$ Hz for a mere ≈ 0.15 s before the chirp. After the chirp, both the ML and NR templates fall rapidly down to the noise level. The result is that the GW150914 signal is visible only for approximately 0.15 – 0.2 s. A time interval of 0.2 s corresponds to a frequency resolution 5 Hz. Such poor resolution is not sufficient to ensure a proper match of the template in the frequency domain. In contrast, rematching techniques, based on Eq. (A.2), that maximize the cross-correlation between the strain data and the template for a short 0.2 s record are unaffected by this poor frequency space resolution. In the discussions below we will consider both templates that are rematched using the Fourier methods of [1] and templates that we rematch directly in the time domain as well as the corresponding residuals.

The use of a PSD obtained from 1040 s of data [1] in order to determine the parameters of a template that is only visible for 0.2 s obviously requires the assumption that the noise is stationary. This assumption is known to be violated, and the noise is tainted by non-Gaussian features and non-stationary behavior. In the presence of such deviations from ideal noise, a more conservative approach is to restrict the analysis to short segments in the time domain within which the effects of non-stationarity and non-Gaussianity are potentially less damaging. After bandpassing and notching, the template is largely localized in 200 ms region. We use data from this region alone to perform rematching of the template to the data.

In Figure 4 we summarize the results presented in [1] for the cross correlation of the Hanford and Livingston residuals using their publicly available program. Results are also shown for the NR template in order to provide a more complete picture of cross correlations in the 40 ms time domain surrounding the chirp. This figure also shows the results after rematching both templates to the data as follows.

- The rematching procedure is intended to maximize separately the correlations defined in eq. (A.2) between the Hanford and Livingston strain data and the template.
- The rematching is performed in the 16.25-16.45 s time window with a sampling rate of 16 kHz for all templates considered³.
- The amplitudes and the phase, ϕ_0 , are not fixed; they are to be determined by optimization.
- The results of Hanford rematching are a pixel shift of 0 pixels, a phase correction of $\Delta\phi_0 \approx -0.05$, and an amplitude correction factor of 1.0241.
- The resulting of Livingston rematching are a pixel shift of -2 pixels (-0.125 ms), a phase correction of $\Delta\phi_0 \approx -0.079$, and an amplitude correction factor of 1.0236.

After rematching, we check the cross-correlation coefficient between the bandpassed and notched strain and the template in the 16.25–16.45s window and find an increase from 0.893 to 0.894 for Hanford and an increase from 0.842 to 0.844 for Livingston, which is consistent with our expectation. For Gaussian random noise, which provides the basis for the ML approach, a higher cross-correlation coefficient necessarily means a higher SNR.

Figures 5–6 show the H/L residuals resulting after templates have been subtracted from the strain data. Results are shown for the ML, NR and rematched NR templates. All figures confirm our expectation that the correlations in the precursor and echo time domains are insensitive to the choice of

³Note that the pixel size for the ML template is 0.25 ms. This is why we perform the rematching using a 16 kHz sample rate.

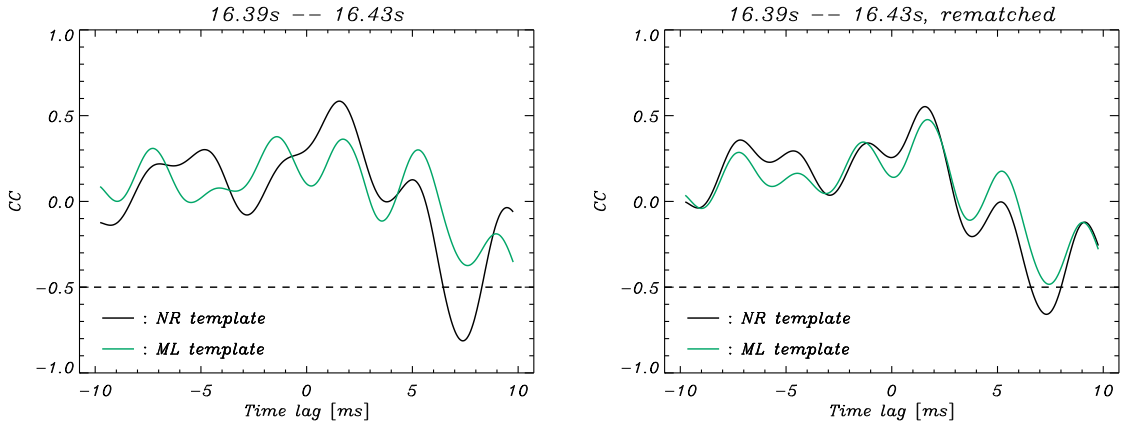


Figure 4. Left panel: Comparison of the ML template residual cross-correlation with that for the NR template. The green curve is identical to Figure 2 in [1]. Right panel: The same residual cross-correlations after rematching. The black and green curves are quite similar; their cross correlation between the black and green curves is 0.95.

template. As shown in [2], these regions are characterized by cross-correlation coefficients on the order of 0.6–0.7. In the chirp domain the structure of the residuals for the rematched ML and rematched NR templates are more similar in spite of the fact that they are significantly different for the non-rematched case.

4 Evaluation of the significance of residual correlations

In our view, the significance estimator used by [1] is both biased and counterintuitive. In Section 4.1, we explain why this is so and use a simple but more robust estimator to calculate the significance. In Section 4.2 we then use the estimator of [1] with necessary corrections to obtain results that can be compared with the results of [1]. Moreover, by comparing the significances estimated in Section 4.1 and Section 4.2 (with corrections), we see that they are in good agreement and that information regarding the peak position is of dominant importance. This will be further illustrated in Appendix B.

4.1 More robust estimation of the significance of residual correlation

The most important feature of the residual correlation is that it appears with a time lag identical to that of the GW event itself. Since the physically allowed time lag range is ± 10 ms, a robust estimation of the probability of the “time lag coincidence” is simply⁴

$$p = 2\Delta t/20, \quad (4.1)$$

where Δt (in ms) is the distance between the positions of the lowest points of the residual and template cross correlations. Eq. (4.1) also has the considerable advantage that it is correct even for non-stationary and non-Gaussian noise provided only that noise in the Hanford and Livingston noises is independent. To illustrate the stability of this estimator, we observe that in Figure 3, 99.8% of the rematched residual correlations (right panel) have their lowest points clustered between 7–8 ms. Even without rematching (left panel), 75% of them are still clustered in this range.

⁴Strictly speaking, the p -value given by eq. (4.1) should be combined with the amplitude of the lowest point to give a complete estimation. However, we have confirmed that this introduces only minor corrections of relatively 10–20%, e.g., a change 4% to 3.6%. Thus, for simplicity, we ignore this correction here.

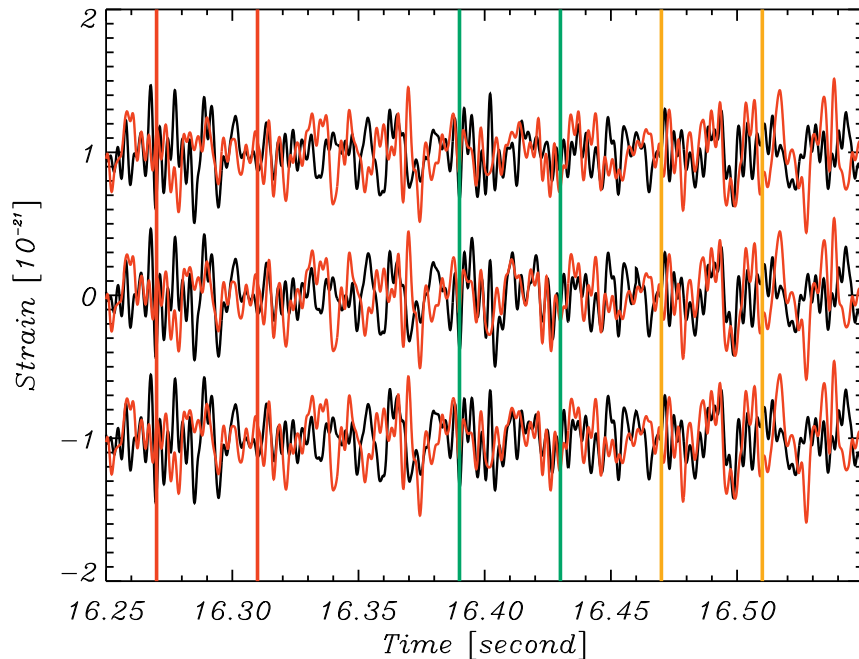


Figure 5. The Hanford (black) and Livingston (red) residuals for the ML template (top), NR template (middle), and the rematched NR template (bottom). The 16.39–16.43 region (green), the precursor region (red) and the echo domain (yellow) are also shown. (See Appendix G and Figure 24 of [2] for details.) Note that Livingston residuals have been shifted by 7 ms and inverted. All residuals have been bandpassed into the frequency range $35 \leq f \leq 350$ Hz.

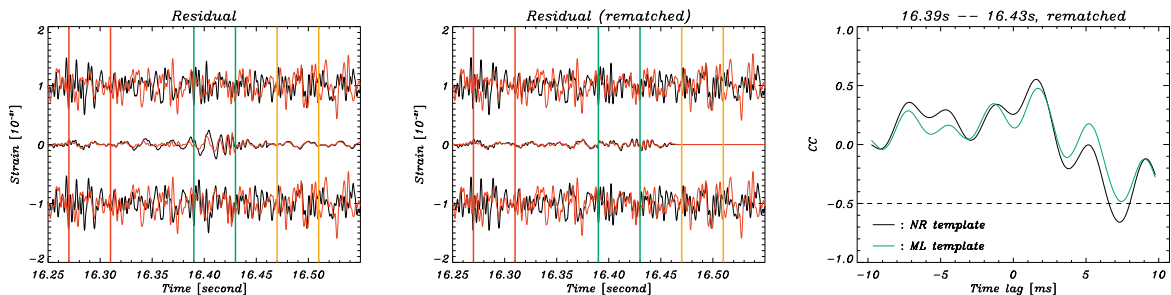


Figure 6. Left panel: The Hanford (black) and Livingston (red) residuals without rematching. The upper plot is for ML and the lower for NR. The middle curve is the difference between them. Middle panel: The same as the left panel but for rematched templates. Livingston residuals have again been shifted by 7 ms and inverted. All residuals have been bandpassed into the frequency range $35 \leq f \leq 350$ Hz. Right panel: the H/L cross-correlation coefficients in the 40 ms chirp domain after rematching. The same as the right panel of Figure 4. Black for ML and green for NR. The cross-correlation between the black and green curves is 0.95.

For the case of the ML template without rematching, Δt is less than 0.4 ms. Thus, from eq. (4.1), the probability of “time lag coincidence” is 4%. When rematching is performed, Δt is reduced to 0.06 ms, and the probability is less than 1%. However, in [1] the probability is given at about 40%, which is completely counterintuitive. This strongly suggests that the estimator used in [1] is significantly

biased.

In Figure 5 of [1], the authors performed an arbitrary modification of the chirp window with the aim of demonstrating that the residual correlation is insignificant. Such an arbitrary choice is not sufficient to support their claim. However, it is still useful to consider modifications of the window chosen. A more reasonable test of this kind can be carried out as follows. We allow the window to start at 16.38, 16.39 or 16.40 seconds, and to end at 16.43, 16.44 or 16.45 seconds. The combinations give 9 different windows at various positions and with various lengths between 30 and 70 ms. Residual correlations have been calculated for all 9 cases (yellow) as well as their average (black), as shown in Figure 7. Apparently this 9-window average estimation is much more reliable than the arbitrary choice in [1]. Before rematching, Δt is found to be about 0.2 ms, corresponds to $p = 2\%$, whereas after rematching, Δt is less than 0.06 ms, corresponding to $p < 1\%$. Later in Section 4.2.2, the same 9-window case is reevaluated using the corrected estimator of [1], and the same 1% probability is found.

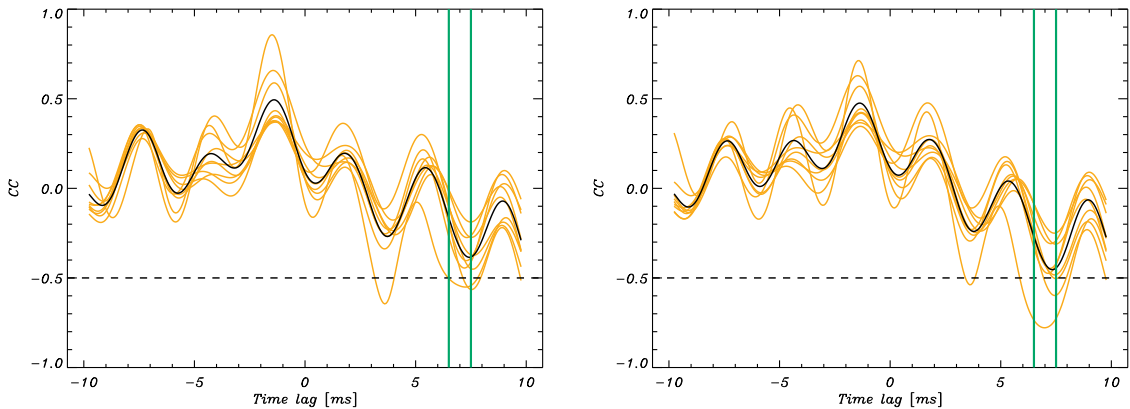


Figure 7. Residual correlations for 9 windows with the windows starting from 16.38, 16.39 and 16.40s, and end at 16.43, 16.44, 16.45s, respectively. The average of 9 windows is plotted in black. Left: no rematching, right: with rematching.

4.2 Calculations with the old estimator

In the event that one elects to use the significance estimator of [1], at least two adjustments are required. Without such corrections, the results will be strongly biased. These include:

1. To obtain a reliable p-value for the observed residual cross-correlation, a correction factor of roughly 0.5 should be applied because we are interested in the significance of the physically meaningful cross correlation including its sign and not the significance of the absolute value of the cross correlation as in [1].
2. To obtain a reliable p-value for the observed residual cross-correlation, at least two points should be considered: a) The local minimum in the 6.5–7.5 ms window as given by simulation is lower than that obtained with real data, and b) The global minimum in the entire ± 10 ms range lies in the same 6.5–7.5 ms window. Unfortunately, in [1] only point a) is considered and b) is completely ignored. This provides another indication that these results are biased.

After considering both corrections, the resulting probability, even with the estimator of [1], will decrease by roughly one order of magnitude and become consistent with the results obtained in Section 4.1.

In fact, even the choice to use the 6.5–7.5 ms is based on the a priori assumption that one already knows that the true time lag is 7 ms. A more natural choice might be to consider Δt as used in eq. (4.1).

4.2.1 Example of varying the window position

In our previous work [2], the window used for the calculation of the residual correlation was 16.39–16.43s. However, we also noticed that this position is somewhat more sensitive to uncertainties in the choice of template than a slightly shifted window running from 16.40–16.44s. For convenience, we will refer to the original window as “chirp A” and the second as “chirp B”. We have used the rematched ML template and residuals to calculate the residual correlation for these windows, and the resulting residual correlations are shown in Figure 8 where the maximum anticorrelations are seen to be -0.48 and -0.60 respectively.

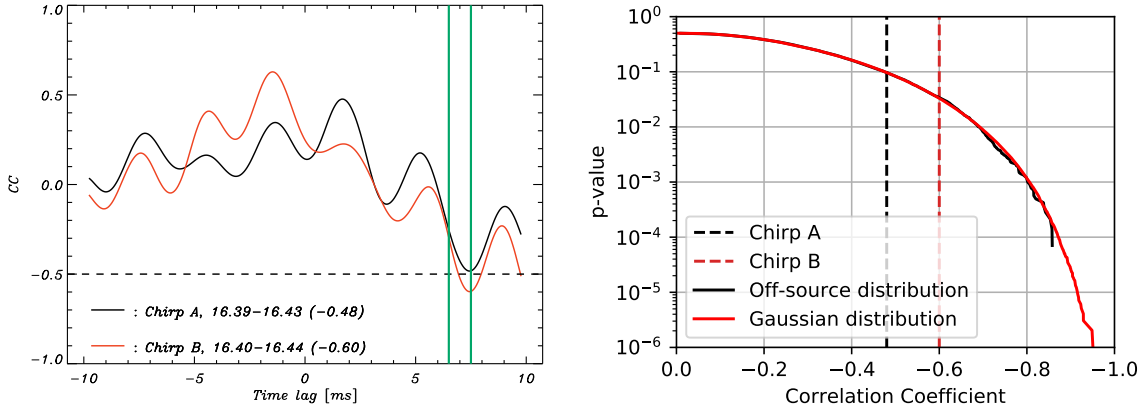


Figure 8. Left panel: The H/L residual correlation using the rematched templates and residuals for the chirp A position (16.39s–16.43s) and the chirp B position (16.40s–16.44s). Right panel: The p-value as a function of the residual correlation reproduced from [1] with the inclusion of the proper factor of 1/2 as discussed in the text. The vertical lines indicate the cross-correlations found for chirp A and chirp B.

In [1], the authors presented a significance estimation of the residual correlation by simulation. However, as mentioned above, they consider only the amplitude but ignore the sign. When the sign of the correlation is correctly taken into consideration, the p-value given in their Figure 3 should be multiplied by a factor of 0.5. We reproduce their Figure 3 as the right panel of Figure 8 including this factor and indicate the residual correlations found at the precursor, chirp A and chirp B positions. We see that the residual correlations for the chirp B window has a significance of $p_B \approx 4\%$. If the position of the lowest point is taken into account, the probability will further decrease.

4.2.2 Significance estimation with 9 window average

As mentioned above and in Section 4.1, one should allow the window position and size to change in a way that is more reasonable than the arbitrary choice in Figure 5 of [1]. In Section 4.1, we used the average of 9 windows to give a more robust estimation. Here we use the same 9-windows and the corrected estimator as described at the beginning of Section 4.2 to re-calculate the significance. The resulting p-value is 1%, which is consistent with the result for 9-windows using eq. (4.1). Therefore, we conclude that, with the use of the ML template, the probability of getting the observed residual correlation in the chirp domain by chance is less than 1%.

4.2.3 Investigation of the RMS peaks

In our previous work [2], the positions of the precursor and echo were detected with a running window calculation of the H/L residual correlation. These features of the noise can also be verified by the running

window RMS test, defined in eq. (4.2) of [2]. Note that this RMS test is independent of the test performed in [2]: The RMS focuses on amplitudes; the test performed in [2] depends only on morphology.

The RMS test is performed in the following way. We take a 20 ms running window⁵ along the Hanford data and the Livingston data (shifted by 7 ms and inverted). For each window, we calculate the joint RMS as

$$\delta(t) = \frac{1}{n} \sqrt{\left(\sum_{i=1}^n H_i(t)^2 \right) \cdot \left(\sum_{i=1}^n L_i(t)^2 \right)}, \quad (4.2)$$

where t is the start time of the window, i is the index of the data points $H_i(t)$ and $L_i(t)$, and n is the total number of points in the window. Figure 9 shows a plot of δ as a function of the time, t , of the left boundary of the window. From this figure we see that the precursor and echo windows correspond not only to regions of morphological similarity [2] but also (and independently) to local regions of joint signal strength. It should also be noticed that, even though the GW event is effectively finished after 16.45 seconds, the bandpassed and notched template continues to show some signal as can be seen from the difference between the black and red lines in Figure 9. (This effect is not visible for the NR template because the length of this template is only 260 ms.) The difference between the red and blue lines in the chirp domain is also noteworthy because it shows that, unlike the NR template, the ML template “absorbs” much more power and introduces significant inhomogeneities (i.e., very low amplitudes) in $\delta(t)$ in the chirp domain. This effect can also be seen in Figure 13 in which comparable results are obtained when the difference between the two GW templates is rescaled by a factor of 5.

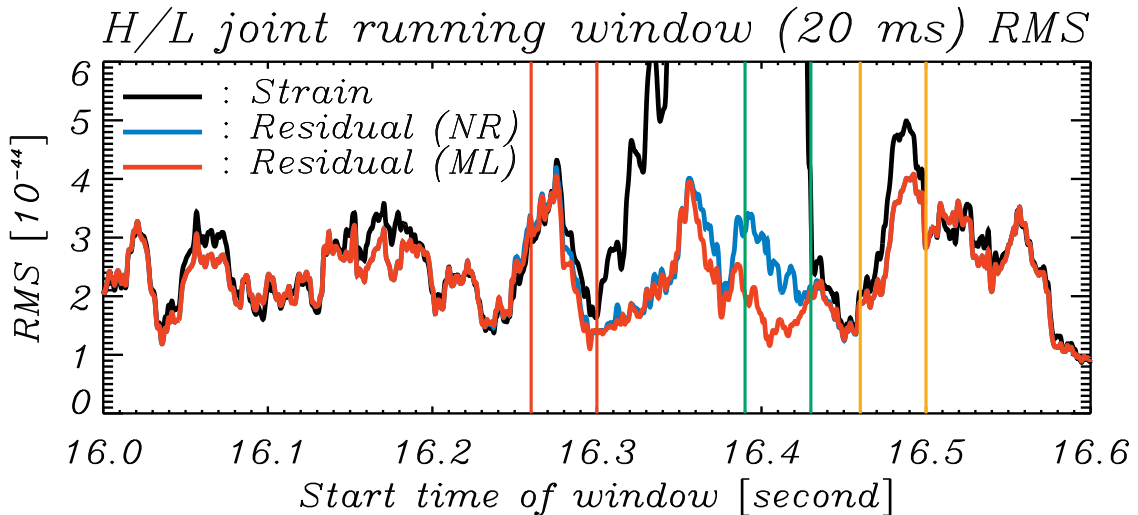


Figure 9. The Hanford and Livingston joint RMS δ calculated for 20 ms running windows using eq. (4.2). The black curve is for the H/L strain (template not removed), the red curve is for the residuals calculated with ML template, and the blue curve is for the residuals calculated with the NR template (neither rematched). The precursor and echo windows are indicated by vertical lines. Since the x -axis denotes the left boundary of the window, we shift the marks by a half-window to the left to represent the effective region more accurately.

⁵For a 40 ms window, 10 ms are excluded from each side in order to avoid edge effects when calculating the residual correlation. The remainder will thus be of 20 ms.

5 Uncertainties in the maximum likelihood method

It is obvious that no fit to data can be considered to be complete until a reliable analysis of the associated uncertainties has been performed. The importance of such an analysis is even greater when the resulting parameters are presumed to have physical significance. Consider, for example, Figure 2 that shows the amplitude of the spin of the larger-mass black hole (upper panel) and the right ascension angle, ra . The former is an intrinsic property of a BH system; the latter determines the sky location of the presumed BBH system. The scatter plots show that each of these parameters can assume essentially any of its possible values. The single point of maximum likelihood selects only one point. The questions are thus: What are the best values for these parameters, what are their uncertainties, and are these uncertainties correlated? Since [1] does not address these issues, we will try to suggest some answers here.

It is important to understand the relation between the strain data (s), the GW signal (h), and the noise ($n = s - h$). The SNR, ρ , used in [1] is given as

$$\rho = \frac{\langle s|h \rangle}{\sqrt{\langle h|h \rangle}} \quad (5.1)$$

with

$$\langle s|h \rangle = 4 \text{Re} \int \frac{s^*(f)h(f)}{S_n(f)} df. \quad (5.2)$$

Here, $S_n(f)$ is the power spectral density of the noise. The log-likelihood for Bayesian inference used by LIGO is

$$\log(L) = -\frac{1}{2} \langle s - h | s - h \rangle, \quad (5.3)$$

which can be converted to $\rho^2/2$ with a proper offset. (The horizontal axis in Figure 2 is $\rho^2/2$.) It was shown [9] that the variance of the log-likelihood associated with different noise realizations is 1.⁶ However, in reality, the log-likelihood should be treated with care. For example, 75% of the points in the MCMC chain have higher SNR than 24, the officially reported SNR of GW150914 [3], thus there is no reason to reject any them. Meanwhile, in the new MCMC chain (see Table 1 and [6]), the mean log-likelihood is lower than the mean of the old chain by 2. Such a difference is about 200 time bigger than the expected fluctuation by chance, assuming Gaussian stationary noise. Finally, as pointed out in Figure 2, a few points look suspicious, and they are unfortunately the ones with highest likelihoods.

In summary, except for some suspicious points, the majority of the MCMC chain should be either all rejected, or all accepted. There is no reason to regard the single ML template as best or most reliable, especially when it and its kind show significant differences from the remainder of the chain. Rather, each of the 37,240 templates represented in Figure 2 is an equally valid best-template candidate. Thus, the results of Figure 2 and Figure 3 provide an illustration of the uncertainties that should be associated with parameter determination and residual correlations (respectively) when adopting the maximum likelihood approach. Consideration of such an extended family of templates would necessarily lead to an increased uncertainty in the determination of parameters and residual correlations due to the MCMC approach. This somewhat pessimistic conclusion is supported by the results shown in Table 1 where a change in the SNR of 0.10% is sufficient to cause significant changes in the template parameters.

⁶This derivation makes the assumption of colored Gaussian noise, but the result has been validated empirically as a good approximation for real detector noise. More seriously, the derivation also assumes that $\langle n|h \rangle = 0$, which is strictly valid only for the maximum likelihood template, and constitutes a “higher-order” correction otherwise.

6 Conclusion

In this work, we have discussed the properties of the noise residuals for GW150914 based on the maximum likelihood template used by [1]. We have paid attention to how residual correlations depend on the template adopted for the description of this event. In particular, we have considered the “maximum likelihood” template of [1] with extreme spin and the original low-spin template from [3]. We have shown that the assertion in [1] that “there are no statistically significant correlations between the noise residuals of the two detectors at the time of GW150914” is incorrect. Specifically, we have demonstrated that the apparent statistical insignificance of the Hanford/Livingston residual correlations in the 40 ms chirp domain is associated with inadequacies in the ML template. After rematching ML and NR templates to the data, the residual correlations for these templates converge to 0.50–0.60 in the chirp domain. A study of various window positions and widths in the provides a more reliable estimation of residual correlations in the vicinity of the GW150914 chirp and suggests that the probability that these noise correlations are genuine is roughly 0.99 (Section 4.1 and 4.2.2).

More seriously, the results of Figures 2 and 3 suggest that the decision to focus on the single template with maximum likelihood is flawed in principle. As noted in Section 2, every one of the 37,240 templates shown in these figures has a high likelihood. It is natural to expect that the templates of highest likelihood will be centrally placed among these templates. Instead, the results reveal a considerable tension in which the parameters of the ML template are not consistent with those that characterize the vast majority of the high-likelihood templates. In this regard, see also the large changes in the templates presented in Table 1 that arise from a truly insignificant 0.1% change in the likelihood. This situation is particularly dangerous since the parameters all have names that invite the reader to attach physical significance to their numerical values. Our physical understanding of GW150914 depends critically on whether the black holes presumed to be involved have the low spins suggested in [3] or the ultrarelativistic spins of [1]. The difficulty lies in the fact that the morphology of the waveforms associated with BBH mergers are remarkably insensitive to the choice of specific parameter values. The strength and importance of this near-degeneracy was considered previously in some detail in [7] but is largely ignored in most discussions of LIGO’s results. Unfortunately, this situation is further complicated by the presence of six adjustable extrinsic parameters that have nothing to do with the intrinsic properties of a BBH system⁷. The appropriate response to these concerns should be a careful analysis of the uncertainties associated with the various intrinsic and extrinsic parameters contained in the waveform. Unfortunately, no suitable estimate of parameter uncertainties is provided in [1] or elsewhere.

Finally, we wish to stress that the present manuscript should not be regarded as either an endorsement of or a challenge to the interpretation of GW150914 as a BBH merger or any other manifestation of gravitational waves. In our view, the physical interpretation of this event remains open. In this sense, we remain convinced that data must be analyzed and a best common signal determined without a priori biases and preconceptions before theoretical models are invoked. It is a truism that, if gravitational waves are all you look for, gravitational waves are all you will ever find.

7 Acknowledgement.

We would like to thank the authors of [1], Duncan A. Brown, Collin D. Capano, Alex B. Nielsen, and Alexander H. Nitz, for their willingness to exchange computer programs and data files. We also thank James Patrick Creswell and Sebastian von Hausegger for helpful and stimulating discussions. This work

⁷In this regard, note from Figure 2 that the right ascension angle, α , is not well determined. As a consequence the sky location of GW150914 cannot be specified with useful accuracy.

has made use of the LIGO software package and data. Our research was funded in part by the Danish National Research Foundation (DNRF) and by Villum Fonden through the Deep Space project. Hao Liu is supported by the Youth Innovation Promotion Association, CAS.

A The Pearson cross-correlator for LIGO noise

The cross correlation coefficient between two data sets, $x(t)$ and $y(t)$, at time t with a time delay τ and window width w is given by

$$C(t, \tau, w, t) = \text{Corr}(x_{t+\tau}^{t+\tau+w}, y_t^{t+w}). \quad (\text{A.1})$$

Here, $\text{Corr}(x, y)$ is the Pearson cross-correlation coefficient [10] between two records x and y defined as

$$\text{Corr}(x, y) = \frac{\sum (x - \bar{x})(y - \bar{y})}{\sqrt{\sum (x - \bar{x})^2 \cdot \sum (y - \bar{y})^2}}, \quad (\text{A.2})$$

where the sums extend over all entries contained in the time interval, w , considered and where \bar{x} and \bar{y} are the corresponding average values of the entries in x and y , respectively.

B A toy model of residuals

In this section we present a toy model of how the non-stationarity of the noise residuals can affect the significance of the amplitude of $C(\tau)$ relative to the importance of the characteristic time lag τ for their correlations.

Suppose that the strain data for Hanford and Livingston are modeled as

$$\begin{aligned} S_H(t) &= W_H(t) \otimes G(t) + n_H(t), \\ S_L(t) &= W_L(t) \otimes G(t + \tau) + n_L(t), \end{aligned} \quad (\text{B.1})$$

where $G(t)$ is the true signal, W is a projection operator (including a transfer function), the operator \otimes denotes a convolution, and $n(t)$ is noise for Hanford and Livingston. Suppose that we use a template, $h(t)$, to fit the observational data of eq. (B.1). In general, this fitting means that

$$\begin{aligned} S_H(t) &= W_H \otimes h(t) + W_H(t) \otimes [G(t) - h(t)] + n_H(t), \\ S_L(t) &= W_L(t) \otimes h(t) + W_L(t) \otimes [G(t + \tau) - h(t + \tau)] + n_L(t). \end{aligned} \quad (\text{B.2})$$

Here, the noise residuals are given as

$$\begin{aligned} R_H(t) &= W_H(t) \otimes [G(t) - h(t)] + n_H(t), \\ R_L(t) &= W_L(t) \otimes [G(t + \tau) - h(t + \tau)] + n_L(t). \end{aligned} \quad (\text{B.3})$$

Thus, the cross-correlation between the residuals, R_H and R_L , from Eq. (A.2) contains the chance correlations for the Hanford and Livingston noise and the residuals between the true signal and the template. Note that the last term is already correlated with the time lag τ . This model clearly illustrates the non-stationarity and non-Gaussianity of the residuals for a time domain in the vicinity of the signal even if the noise terms, n_H and n_L , are Gaussian and stationary.

In order to investigate the properties of the residual correlations, $C(\tau)$, for this model, we use the 4096 s, bandpassed ($35 \leq f \leq 350$ Hz) and notched strain data given at [4], which are identical to those adopted in [1]. We consider 50 disjoint domains of length 0.2 s for times well after the GW150914 event

and inject in each of them the signal G_{losc} with an H/L time lag of $\tau = 7$ ms as given by the LOSC template for GW150914 with masses $m_1 = 41.743M_\odot$ and $m_2 = 29.237M_\odot$ and spins, $spin_1 = 0.355$ and $spin_2 = -0.769$. These 50 domains mimic a statistical ensemble with a signal of G_{losc} and different realizations of genuine LIGO noise.

For the reconstruction of the signal in each of these 50 domains we use the ML template rematched to the simulated data. It is useful to characterize the mismatch of the “signal” and the template by functions $r_{\text{H/L}}$, for Hanford and Livingston, respectively:

$$r = -f (h_{ML}(t) - h_{\text{losc}}(t)) \quad (\text{B.4})$$

where the parameter f is chosen such that $|r|$ is much less than $|h_{\text{losc}}|$ and $|h_{ML}|$. In this toy model all statistical properties of the noise and the residuals are known. For $f = 0$ the $C(\tau)$ from eq. (A.2) corresponds to the pure noise correlations, for $f = 1$ we get the contribution from the difference of the templates plus noise and, formally, for $f \rightarrow \infty$ we should see that $C \rightarrow -1$ for $\tau = 7$ ms in each domain.

Figure 10 shows the difference between the (bandpassed and notched) LOSC and ML templates. These templates are matched to the ML template used as a proxy for the GW150914 signal. For compar-

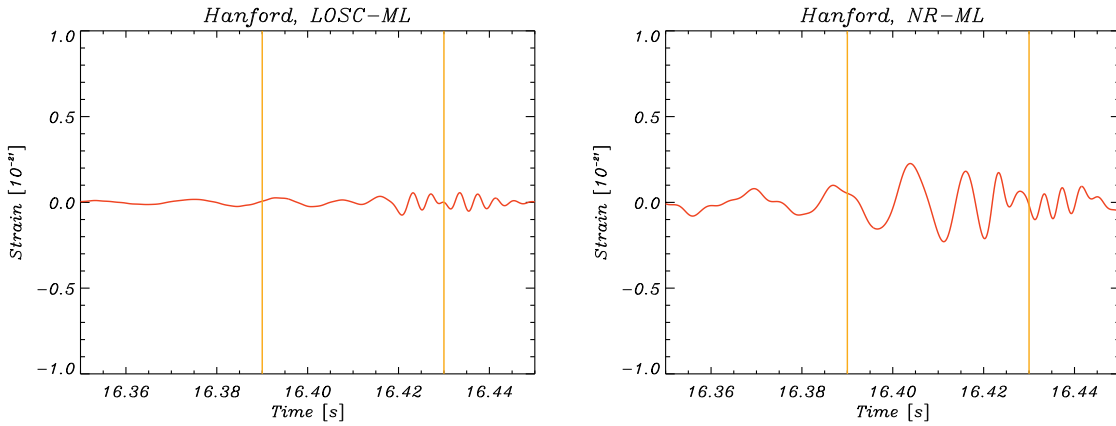


Figure 10. Left panel. The difference between ML and LOSC templates. Right panel. Same as the left but for ML and NR templates

ison, the figure also shows the difference between NR and ML templates with the same normalisation. The difference between NR and ML templates is seen to be roughly twice the size of the difference between the ML and LOSC templates. Note the position of the peaks is different in the two panels of this figure.

In Figure 11 the left panel corresponds to the pure chance correlations of the noise and the right panel show the residual correlations for the choice $f = 1$. Note that the choice $f = 1$ corresponds to the case for which the signal (in the form of the LOSC template) is fitted by the ML template. Let us focus on the time lag of the residual correlations in the vicinity of $\tau = 7$ ms. For $f = 0$, one sees a negative peak in this domain with $C \simeq -0.75$. (See the green line in Figure 11). According to Figure 8, the corresponding probability for finding a peak of this size is $P \simeq 0.01$. For the choice $f = 1$, the amplitude of this peak becomes $C \simeq -0.9$ a corresponding probability of $P \simeq 10^{-4}$ according to Figure 8. The same tendency can be seen for the yellow positive peak at $\tau \simeq -(3.5)$ ms. For $f = 0$ the chance noise correlations are $C(\tau \simeq -3.5) \simeq 0.8$ with a corresponding probability of $P \simeq 10^{-3}$ which decreases to $P \simeq 2 \times 10^{-4}$ for $f = 1$.

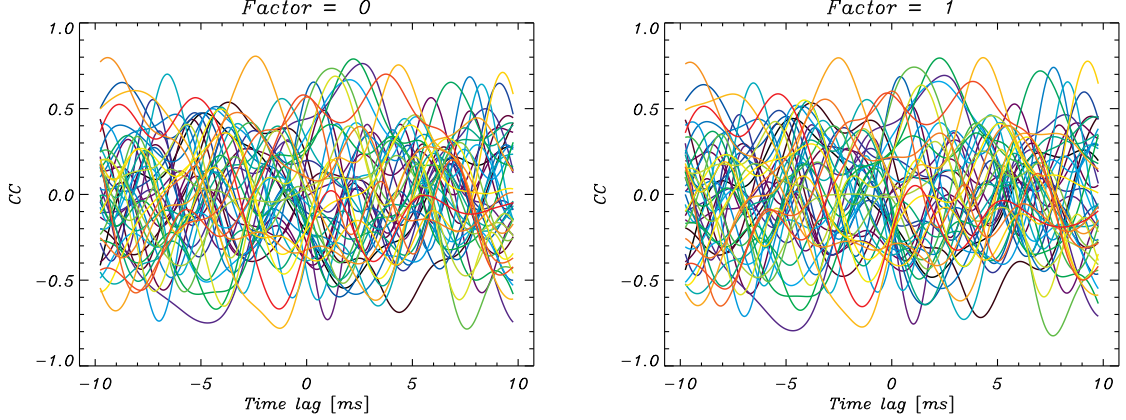


Figure 11. The residual correlation, $C(\tau)$ for $f = 0$ (left panel) and $f = 1$ (right panel).

Thus, in the toy model considered here, we can trace the influence of the mismatch of signal and template on the probability of the peak correlations. Usually, a mismatch between template and signal leads to a stronger residual (anti)correlation than that found for chance noise correlations alone. However, this is not necessarily the case when the genuine signal is unknown, as is the case in the chirp domain of the GW150914 event.

B.1 Residuals correlations for the high amplitude case.

In the toy model presented above the true signal is given by the LOSC template is approximated by the ML template. In this case, the “exact” solution to the problem of residual correlations is given by eq. (B.2) with $f = 1$. Let us now assume that we have no information regarding chance correlations, so that we attempt to fit the data using a combination of the ML template and the residuals, r from eq. (B.4), with $f > 1$. Note that the residuals r have a characteristic time lag $\tau \simeq 7$ ms. Figure 12 shows $C(\tau)$ for $f = 3, 5$, and 10 as a function of $|\tau| \leq 10$ ms.

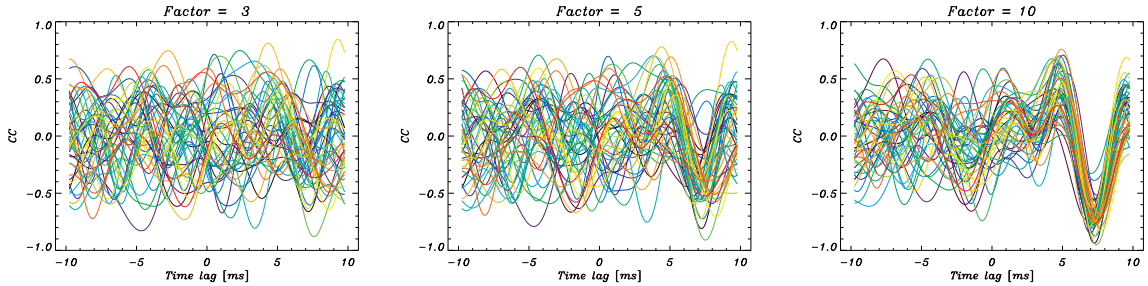


Figure 12. The residual correlation $C(\tau)$ for $f = 3$ (left panel), $f = 5$ (middle panel) and $f = 10$ mode (right panel).

We see that, as the residuals, r become larger, almost all of the cross-correlation functions collapse to asymptotic values, $C(\tau)$, with clearly established time lag 7 ms. Moreover, the comparison between $f = 5$ and $f = 10$ models presented in Figure 13, clearly illustrates the transition of the chance correlations from positive to negative values in the domain $\tau = 7$ ms (See the blue and green lines in this domain.) It is worth noting that the term $f [h_{\text{losc}}(t) - h_{\text{ML}}(t)]$ becomes roughly comparable to the residuals (black line) when $f = 5$. This collapse of correlations is due to the increasing amplitude of

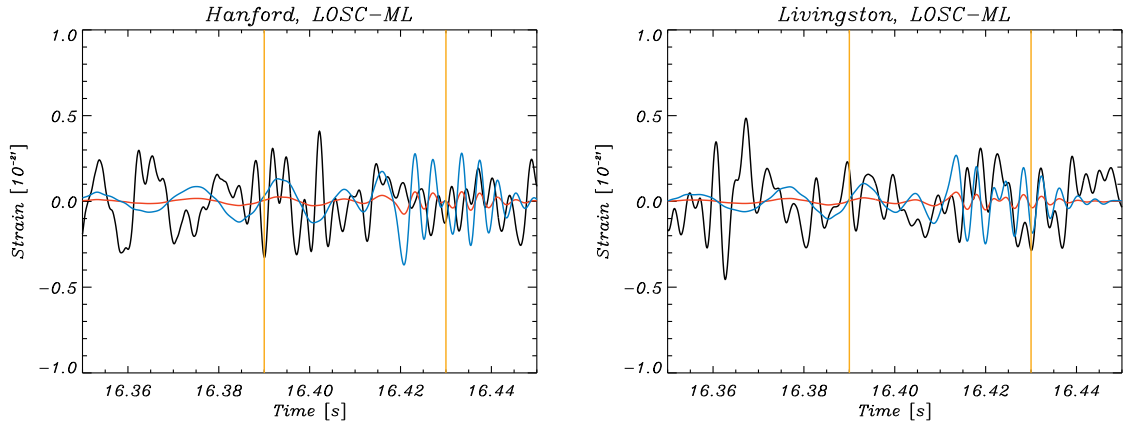


Figure 13. Comparison of the Hanford (left) and Livingston (right) ML template residuals (black) with the $f [h_{losc}(t) - h_{ML}(t)]$ term, where $f = 1$ and 5 respectively (red and blue). Two yellow vertical lines indicate the position of chirp domain.

the residuals relative to the amplitude of the noise that makes the residual term more non-stationary and non-Gaussian. At the same time, the application of the Gaussian statistics from the right panel of Figure 8 will give us a completely misleading result. It follows from the right panel of Figure 8 that the corresponding chance probability is localized in the domain $0.1 - 1$.

It is worth noting that the effect of the collapse of the residual correlations, described with our toy model, is very general. For unknown signal, $g(t)$, the noise residuals are given by eq. (B.4), where both g and h have the same time lag τ . Thus, when the term $\propto (g - h)$ is close to the noise term $n(t)$, we will see the beginning of the collapse of $C(\tau)$ around $\tau \simeq 7$ ms. The residuals are non-stationary and non-Gaussian, but the amplitude of $C(\tau)$ can be relatively small ($C(\tau \simeq 7ms) \simeq 0 - 0.5$). Once again, assuming Gaussianity of the residuals and using Figure 8 one will conclude that this particular realisation of the residuals is very likely, which is obviously not the case.

References

- [1] A. B. Nielsen, A. H. Nitz, C. D. Capano and D. A. Brown, *Investigating the noise residuals around the gravitational wave event GW150914*, *Journal of Cosmology and Astro-Particle Physics* **2019** (Feb, 2019) 019, [1811.04071].
- [2] J. Creswell, S. von Hausegger, A. D. Jackson, H. Liu and P. Naselsky, *On the time lags of the LIGO signals*, *JCAP* **8** (Aug., 2017) 013, [1706.04191].
- [3] LIGO SCIENTIFIC COLLABORATION AND VIRGO COLLABORATION collaboration, B. P. Abbott, R. Abbott, T. D. Abbott, M. R. Abernathy, F. Acernese, K. Ackley et al., *Observation of gravitational waves from a binary black hole merger*, *Phys. Rev. Lett.* **116** (Feb, 2016) 061102.
- [4] “NBI site for gravitational waves.” <http://www.nbi.ku.dk/gravitational-waves/>.
- [5] C. M. Biwer, C. D. Capano, S. De, M. Cabero, D. A. Brown, A. H. Nitz et al., *PyCBC Inference: A Python-based parameter estimation toolkit for compact binary coalescence signals*, *arXiv e-prints* (July, 2018) arXiv:1807.10312, [1807.10312].
- [6] C. M. Biwer, C. D. Capano, S. De, M. Cabero, D. A. Brown, A. H. Nitz et al., “Github repository of the mcmc chain data file.” <https://github.com/gwastro/pycbc-inference-paper/commits/master/posteriors/GW150914>.

- [7] J. Creswell, H. Liu, A. D. Jackson, S. von Hausegger and P. Naselsky, *Degeneracy of gravitational waveforms in the context of GW150914*, *Journal of Cosmology and Astro-Particle Physics* **2018** (Mar, 2018) 007, [[1803.02350](#)].
- [8] D. A. Brown, *Searching for Gravitational Radiation from Binary Black Hole MACHOs in the Galactic Halo*, Ph.D. thesis, PhD Thesis, 2007, May, 2007.
- [9] B. Allen, W. G. Anderson, P. R. Brady, D. A. Brown and J. D. E. Creighton, *Findchirp: An algorithm for detection of gravitational waves from inspiraling compact binaries*, *Phys. Rev. D* **85** (Jun, 2012) 122006.
- [10] K. Pearson, *Note on Regression and Inheritance in the Case of Two Parents*, *Proceedings of the Royal Society of London Series I* **58** (1895) 240–242.